24th INTERNATIONAL CONGRESS ON SOUND AND VIBRATION
23–27 July 2017, London

THE EFFECT OF ENCLOSURE COUPLING ON A DUAL-LAYER LINEAR LOUDSPEAKER ARRAY

Jordan Cheer
University of Southampton, Institute of Sound and Vibration Research, Highfield, Southampton, UK
email: j.cheer@soton.ac.uk

Loudspeaker arrays are increasingly being used in a variety of applications where there is a restriction on the electrical power consumption and the array must be robust to changes in the acoustic environment. Previous work has demonstrated that the efficiency and robustness of a two-source endfire loudspeaker array can be improved by acoustically coupling the two loudspeakers via a common enclosure. This paper presents an investigation into the effects of using acoustically coupled enclosures in a dual-layer linear loudspeaker array. Three different dual-layer array designs will be compared. In the first configuration each loudspeaker is mounted in its own enclosure and, therefore, there is no internal coupling between the loudspeakers. In the second configuration, each pair of front-to-back loudspeakers in the dual layer array are coupled via a common enclosure. Finally, in the third configuration all of the loudspeakers are coupled via a single enclosure. The performance of the three array configurations is investigated in terms of the acoustic contrast, the array effort, or electrical power, and the robustness to variations in the electroacoustic responses. Through this investigation it is shown that an increase in efficiency can be achieved by coupling the front-to-back pairs of loudspeakers in the dual-layer linear array.

Keywords: Personal Audio, Sound Field Control, Loudspeaker Array, Acoustic Coupling

1. Introduction

The generation of personal sound zones allows multiple listeners in a common space to receive personalised audio content without disturbing other occupants of the space. Personal sound zone systems have been developed for a number of applications including mobile devices [1, 2], computer monitors [3], car cabin interiors [4, 5], home entertainment systems [6], and aircraft seats [7]. These systems use arrays of loudspeakers to focus the sound in a particular location, whilst ensuring that the sound level generated in other locations is kept to a minimum. The design of these sound field control systems involves both the design of the physical loudspeaker array geometry, as well as the signal processing strategy that is used to calculate the signals that drive the loudspeakers. A number of different signal processing strategies have been proposed to solve this problem [8, 6, 9, 10, 11, 12] and in practice, the system must reach a trade-off between a number of factors, which include: the acoustic separation, or acoustic contrast, between the listening and quiet zones [8]; the robustness of the system to changes in the acoustic environment [13, 14, 15]; and the audio quality [16].

In the mobile device application, the electrical power required by the loudspeaker array should be kept to a minimum and it is often necessary to employ constraints on the magnitude of the filters to avoid overdriving the loudspeakers and introducing non-linearities [17]. This has generally been achieved using regularisation in the optimisation of the loudspeaker driving signals [13] and this also improves the robustness of the array to uncertainty in the responses [13, 18]. However, regularisation

also limits the directivity, or acoustic contrast of a given loudspeaker array. For the specific case of a two-source endfire array, it has been shown that by coupling the two loudspeakers through a common enclosure it is possible to significantly reduce the required electrical power without reducing the acoustic contrast performance [1]. In [19] the robustness of this system to variations in the electroacoustic responses has been investigated and it has been demonstrated that the acoustically coupled two-source array significantly outperforms the standard uncoupled array in the presence of response uncertainties, even when the electrical power in the uncoupled array is limited to match that of the coupled array.

Although it has been shown that the two-source coupled loudspeaker array is able to achieve a higher level of acoustic contrast than a standard uncoupled array, in many applications it is necessary to use a larger array of loudspeakers to achieve the necessary level of acoustic contrast. In particular, a number of previous studies have used dual-layer loudspeaker arrays to achieve the desired level of performance [10, 20]. This paper, therefore, explores the use of the coupled loudspeaker array proposed in [1] in a dual-layer linear array. In the first section the acoustic contrast control strategy is reviewed. In Section 3 models of the acoustically coupled loudspeaker arrays are derived and in Section 4 they are used to investigate the performance and robustness of the different dual-layer loudspeaker array configurations. Finally, in Section 5 conclusions are drawn.

2. Superdirective Beamforming

As noted in the introduction, a variety of different strategies have been proposed to calculate the signals used to drive the loudspeakers in a superdirective or optimal beamformer with the aim of generating independent personal sound zones. These different methods generally provide some trade-off between the level of separation between the listening and quiet zones and the audio quality in the bright zone. In this instance, although the audio quality is known to be limited, the acoustic contrast control strategy [8] will be employed since it gives the highest level of sound zone separation for a given loudspeaker array and, therefore, provides a consistent basis for comparing the different loudspeaker arrays.

The acoustic contrast can be defined at a single frequency as the ratio of the mean of the squared pressures in the bright, or listening zone, to the mean of the squared pressures in the dark, or quiet zone. If the pressures in the bright and dark zones are defined at N_B and N_D positions respectively, then these pressures can be expressed by the column vectors $\mathbf{p}_B$ and $\mathbf{p}_D$. The acoustic contrast at a single frequency is then [1]

$$C = \frac{N_D \mathbf{p}_B^H \mathbf{p}_B}{N_B \mathbf{p}_D^H \mathbf{p}_D} = \frac{N_D \mathbf{i}^H \mathbf{G}_B^H \mathbf{G}_B \mathbf{i}}{N_B \mathbf{i}^H \mathbf{G}_D^H \mathbf{G}_D \mathbf{i}}, \tag{1}$$

where superscript H is the Hermitian, complex conjugate, transpose; $\mathbf{i}$ is the vector of the L complex signals driving the loudspeakers in the array; and $\mathbf{G}_B$ and $\mathbf{G}_D$ are the matrices of transfer responses between the inputs to the L individual loudspeakers in the array and the N_B and N_D pressure measurement positions in the bright and dark zones respectively. From this ratio it can be seen that the vector of driving signals, $\mathbf{i}$, must be optimised in order to maximise the acoustic contrast.

This optimisation problem can be cast as a constrained quadratic optimisation in which the sum of the squared pressures in the dark zone, $\mathbf{p}_D^H \mathbf{p}_D$, is minimised, subject to the constraint that the sum of the squared pressures in the bright zone, $\mathbf{p}_B^H \mathbf{p}_B$, is held constant with a value B. It is also useful in practice to include an additional constraint such that the array effort, or sum of the squared driving signals, $\mathbf{i}^H \mathbf{i}$, which is proportional to the electrical power, is held constant with a value W. The cost function in this case can be expressed as the Lagrangian [13]

$$J = \mathbf{i}^H \mathbf{G}_D^H \mathbf{G}_D \mathbf{i} + \lambda_B \left(\mathbf{i}^H \mathbf{G}_B^H \mathbf{G}_B \mathbf{i} - B \right) + \lambda_W \left(\mathbf{i}^H \mathbf{i} - W \right), \tag{2}$$

where λ_C and λ_W are the Lagrange multipliers relating to the bright zone and electrical power constraints respectively. The optimal solution is then given by setting the differential of J with respect to

the real and imaginary parts of $\mathbf{i}$ to zero [1, 13] and this gives

$$\lambda_B \mathbf{i} = -\left[\mathbf{G}_D^H \mathbf{G}_D + \lambda_W \mathbf{I}\right]^{-1} \mathbf{G}_B^H \mathbf{G}_B \mathbf{i}. \tag{3}$$

This is a classical eigenvalue problem and the optimal solution for the vector $\mathbf{i}$ is proportional to the eigenvector of $\left[\mathbf{G}_D^H \mathbf{G}_D + \lambda_W \mathbf{I}\right]^{-1} \mathbf{G}_B^H \mathbf{G}_B$ corresponding to its largest eigenvalue, where λ_W has to be set such that the constraint on $\mathbf{i}^H \mathbf{i}$ is satisfied [8, 13]. The absolute value of $\mathbf{i}$ is then determined by setting the Lagrange multiplier, λ_B, such that the constraint on the sum of the squared pressures in the bright zone is fulfilled. In practice, since the sum of the squared driving signals, $\mathbf{i}^H \mathbf{i}$, will also be dependent on λ_B, the selection of the two Lagrange multipliers must be achieved through an iterative process to ensure that both constraints are fulfilled.

In the following investigation, it is assumed that the bright zone is defined by a single pressure evaluation position, as shown by the red circle in Figure 1, whilst the dark zone is defined by the pressures evaluated at the dark circles in Figure 1, which surround the loudspeaker array.

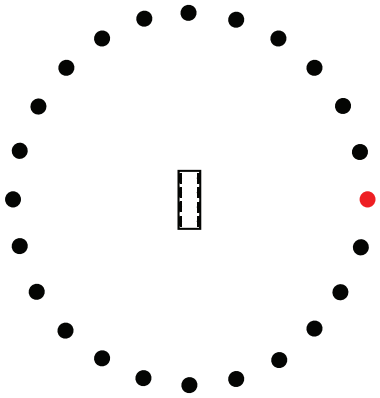

Figure 1: The microphone array geometry: the red circle defines the bright zone and the dark circles define the dark zone.

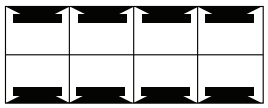

(a) The uncoupled dual-layer array.

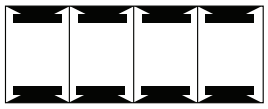

(b) The two-source coupled dual-layer array.

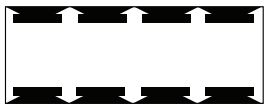

(c) The fully coupled dual-layer array.

Figure 2: The uncoupled (a), two-source coupled (b) and fully coupled (c) dual-layer loudspeaker arrays.

3. Model of the Dual-Layer Loudspeaker Arrays

The two-source loudspeaker array can be implemented using either a single coupled enclosure, or two independent, closed-back enclosures, as described in [1, 19]. In the case of a dual-layer loudspeaker array, three possible enclosure configurations will be considered here as shown in Figure 2. Figure 2a shows the uncoupled dual-layer array, which is consistent with typical array configurations, Figure 2b shows the dual-layer array using two-source coupled enclosures and Figure 2c shows the fully coupled dual-layer array. In each case, the response of the individual loudspeakers will be modified by the coupling between the drivers. As in [1, 19], the coupling can be modelled using a two-port network approach. The two-port network model assumes that the loudspeaker diaphragms act as pistons and the exterior radiation from the individual loudspeakers is then modelled using free field monopole sources. Although these are approximations, previous work has demonstrated that such models provide sufficiently accurate results at low frequencies where the wavelength is large compared to the dimensions of the diaphragm.

The two-port network model described in [1, 19] can be extended to the array of L loudspeakers considered here. The vector of volume velocities produced by the array can be expressed in terms of the vector of driving signals, $\mathbf{i}$, and the effective pressures acting on the diaphragms, $\mathbf{p}$, as

$$\mathbf{q} = \mathbf{S}\mathbf{i} + \mathbf{Y}_{a0}\mathbf{p} \tag{4}$$

where $\mathbf{S}$ and $\mathbf{Y}_{a0}$ are the diagonal matrices of loudspeaker sensitivities and acoustic admittances corresponding to the L loudspeakers respectively. The acoustic admittance matrix is given by

$$\mathbf{Y}_{a0} = \frac{1}{Z_{a0}}\mathbf{I}, \tag{5}$$

where $\mathbf{I}$ is the identity matrix and Z_{a0} is the open-circuit acoustical impedance given by

$$Z_{a0} = \frac{Z_{m0}}{\left(\pi a^2\right)^2} = \frac{R + j\left(\omega M - K/\omega\right)}{\left(\pi a^2\right)^2} \tag{6}$$

where Z_{m0} is the open-circuit mechanical impedance of the loudspeaker, a is the radius of the loudspeaker diaphragm, R is the damping, M is the moving mass and K is the stiffness of the loudspeaker suspension. The loudspeaker sensitivity matrix is given by

$$\mathbf{S} = \frac{T}{Z_{a0}}\mathbf{I} = \frac{Bl_{coil}/\pi a^2}{Z_{a0}}\mathbf{I} \tag{7}$$

where T is the loudspeaker transduction coefficient, B is the magnetic flux density and l_{coil} is the length of the voice coil in the magnet gap.

The vector of effective pressures acting on the diaphragms is given by the difference between the pressure acting on the front of the diaphragms due to the radiated pressures and the pressures acting on the rear of the diaphragms due to the internal coupling, such that

$$\mathbf{p} = \mathbf{Z}_R\mathbf{q} - \mathbf{Z}_L\mathbf{q}, \tag{8}$$

where $\mathbf{Z}_R$ is the matrix of self and mutual radiation impedances and $\mathbf{Z}_L$ is the matrix of input and transfer impedances within the enclosure. In practice, for all three enclosure designs shown in Figure 2, the radiation impedances will be small compared to the load impedances and, therefore, may be neglected, as in [1]. Thus, neglecting the radiation impedances and substituting eq. (8) into eq. (4) and rearranging gives the vector of volume velocities as

$$\mathbf{q} = \left[\mathbf{I} + \mathbf{Y}_{a0}\mathbf{Z}_L\right]^{-1}\mathbf{S}\mathbf{i}. \tag{9}$$

The impedance matrix, $\mathbf{Z}_L$, in eq. (9) determines the difference in behaviour between the three dual-layer loudspeaker array designs. For the uncoupled array shown in Figure 2a, the impedance matrix is diagonal, since there is no cross-coupling between the loudspeakers and is given by

$$\mathbf{Z}_L = \begin{bmatrix} Z_I & 0 & 0 & 0 \\ 0 & Z_I & 0 & 0 \\ 0 & 0 & \ddots & 0 \\ 0 & 0 & 0 & Z_I \end{bmatrix}, \tag{10}$$

where Z_I is the input impedance seen by the loudspeakers. In the case of the two-source coupled array shown in Figure 2b, the impedance matrix is block diagonal, since each loudspeaker is only coupled internally to one other loudspeaker and can thus be written as

$$\mathbf{Z}_L = \begin{bmatrix} \begin{bmatrix} Z_I & Z_C \\ Z_C & Z_I \end{bmatrix} & \mathbf{0} & \mathbf{0} & \mathbf{0} \\ \mathbf{0} & \begin{bmatrix} Z_I & Z_C \\ Z_C & Z_I \end{bmatrix} & \mathbf{0} & \mathbf{0} \\ \mathbf{0} & \mathbf{0} & \ddots & \mathbf{0} \\ \mathbf{0} & \mathbf{0} & \mathbf{0} & \begin{bmatrix} Z_I & Z_C \\ Z_C & Z_I \end{bmatrix} \end{bmatrix}, \tag{11}$$

where Z_I is the input impedance seen the loudspeakers and Z_C describes the coupled between the pairs of coupled loudspeakers. Finally, the impedance matrix that describes the loads acting on the loudspeakers in the fully coupled array shown in Figure 2c is a fully populated matrix given by

$$\mathbf{Z}_L = \begin{bmatrix} Z_I & Z_{C_{1,2}} & \cdots & Z_{C_{1,L}} \\ Z_{C_{2,1}} & Z_I & & \vdots \\ \vdots & & \ddots & Z_{C_{(L-1),L}} \\ Z_{C_{1,L}} & \cdots & Z_{C_{(L-1),L}} & Z_I \end{bmatrix}, \tag{12}$$

where Z_I is the input impedance matrix and $Z_{C_{j,k}}$ is the coupling between the the j-th and k-th loudspeakers in the array.

It should be highlighted that impedance matrices given by eqs. (10), (11) and (12) all have dimensions of $L \times L$ and in each case the value of the input impedance, Z_I, differs due to the difference in the size of the enclosure. The input and coupling impedances in each array can be calculated using a number of different approaches. For example, in [19] they are calculated by assuming that only plane waves propagate in the enclosure, which may be reasonable depending on the dimensions of the enclosure relative the frequency of interest. However, in this case, the input and coupling impedances have been calculated using a modal model of the enclosures in each case, which allows higher order modes to be included.

The pressures that are radiated from the loudspeaker arrays to the bright and dark zones can be calculated as

$$\mathbf{p}_B = \mathbf{Z}_B\mathbf{q} \qquad\qquad \mathbf{p}_D = \mathbf{Z}_D\mathbf{q} \tag{13}$$

where $\mathbf{Z}_B$ and $\mathbf{Z}_D$ are the acoustic transfer impedances between the acoustic volume velocities of the two loudspeakers and the pressures measured at the N_B and N_D microphone locations in the bright and dark zones respectively. Substituting Eq. (9) into Eq. (13) then gives the vectors of bright and dark zone pressures in terms of the loudspeaker driving signals as

$$\mathbf{p}_B = \mathbf{Z}_B \left[\mathbf{I} + \mathbf{Y}_{a0}\mathbf{Z}_L\right]^{-1} \mathbf{Si} \qquad\qquad \mathbf{p}_D = \mathbf{Z}_D \left[\mathbf{I} + \mathbf{Y}_{a0}\mathbf{Z}_L\right]^{-1} \mathbf{Si}. \tag{14}$$

Since the full electroacoustic transfer response matrices, $\mathbf{G}_B$ and $\mathbf{G}_D$ are dependent on the impedance matrix $\mathbf{Z}_L$, which differs for the three enclosure configurations, the optimal driving signals will differ for the fully coupled, two-source coupled and uncoupled dual-layer loudspeaker arrays. The effect of this on both the efficiency and robustness of the arrays will be investigated in the following section.

4. Simulation Results

To compare the performance and robustness of the three dual-layer array configurations shown in Figure 2, the systems will be simulated using the models detailed in the previous section. It has been assumed that each array consists of 8 loudspeakers, as depicted in Figure 2. The assumed loudspeakers have a radius of 1 cm, which gives an overall array length of 8 cm, and the depth of the array, or separation between the two layers, has been set to be 3 cm. The individual enclosures in the uncoupled array therefore have an assumed volume of 6 cm^3, the enclosures in the two-source coupled array have a volume of 12 cm^3 and the fully coupled array has an enclosure volume of 48 cm^3. As expected, this change in the internal volume of the enclosures changes the effective stiffness of the loudspeaker drivers, such that with a larger volume the effective stiffness is lower and the resonance of the loudspeaker occurs at a lower frequency.

4.1 Optimal Performance of the Dual-Layer Arrays

In the first instance, the performance of the three dual-layer arrays, optimised using the acoustic contrast control strategy described by eq. (3), has been calculated using the models described in

the previous section. The Lagrange multiplier corresponding to the constraint on the bright zone sound pressure level, λ_B, has been set so that each array produces a sound pressure level of 60 dB in the bright zone. Figure 3 shows the acoustic contrast and the electrical power required by each array when there are no uncertainties in the electroacoustic responses. The thick dark line in Figure 3a shows the acoustic contrast achieved by the three arrays with no constraint on the array effort, whilst the thin dark line shows the acoustic contrast achieved by the uncoupled array when the array effort is constrained to be no greater than that required by the coupled arrays. Figure 3b shows the electrical power required by the three arrays to achieve the acoustic contrast shown in Figure 3a for the uncoupled array (black line), the two-source coupled array (red line) and the fully coupled array (blue line). From these results it can be seen that at frequency below around 600 Hz, in this case, the coupled arrays provide a significant reduction in the required electrical power, despite achieving the same level of acoustic contrast. In particular, at frequencies below around 250 Hz, the electrical power required by the two arrays with coupled enclosures is around 40 times lower than that required by the uncoupled array. At higher frequencies, the coupled arrays require a higher electrical power than the uncoupled array, as they do not benefit from the higher resonant frequency of the smaller uncoupled cavities. However, the electrical power in this range is negligible in comparison to that required at lower frequencies.

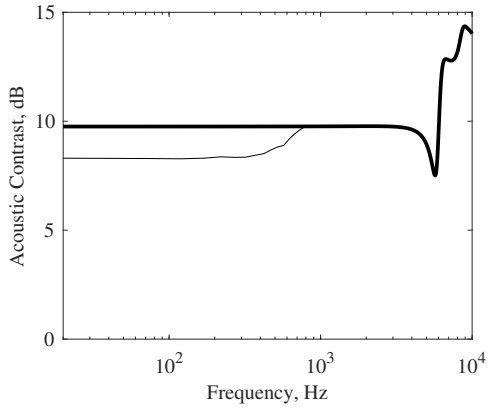

(a) Acoustic contrast of the dual-layer loudspeaker arrays (bold solid line) and the uncoupled array with a constraint on the array effort (thin solid line).

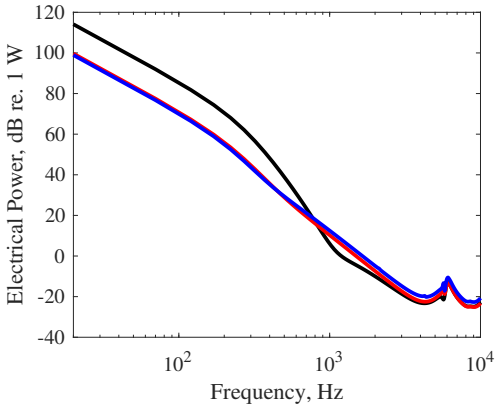

(b) The electrical power required by the uncoupled (bold solid black line), two-source coupled (bold solid red line) and fully coupled (bold solid blue line) loudspeaker arrays.

Figure 3: The acoustic contrast and electrical power of the dual-layer loudspeaker arrays when there is no uncertainty in the electroacoustic responses.

4.2 Robustness to Uncertainties

Although it has been shown that the coupled arrays achieve a reduction in the required electrical power compared to the standard uncoupled array, it is also interesting to consider how the coupling influences the robustness of the array to uncertainties in the electroacoustic responses. To investigate the effect of uncertainties on the array performance it has been assumed that the electroacoustic responses are perturbed a random error, which can be introduced as

$$\hat{\mathbf{G}}_B = \mathbf{G}_B + \boldsymbol{\Delta}\mathbf{G}_B \qquad \hat{\mathbf{G}}_D = \mathbf{G}_D + \boldsymbol{\Delta}\mathbf{G}_D, \tag{15}$$

where $\boldsymbol{\Delta}\mathbf{G}_B$ and $\boldsymbol{\Delta}\mathbf{G}_D$ are matrices of the uncertain components. For the case when it is assumed that the uncertainties are uncorrelated with the unperturbed responses the performance of the three arrays has been calculated for different levels of uncertainties and the results are shown in Figure 4. From these results it can be seen that the coupled loudspeaker arrays, shown by the red and blue dashed

lines, outperform the uncoupled array, shown by the black dashed line, when there are uncertainties in the responses. It is also interesting to observe that when regularisation is used to limit the electrical power used by the uncoupled array to be equal to that used required by the coupled arrays, it can be seen that for the levels of error considered in Figure 4, the coupled arrays continue to outperform the uncoupled array.

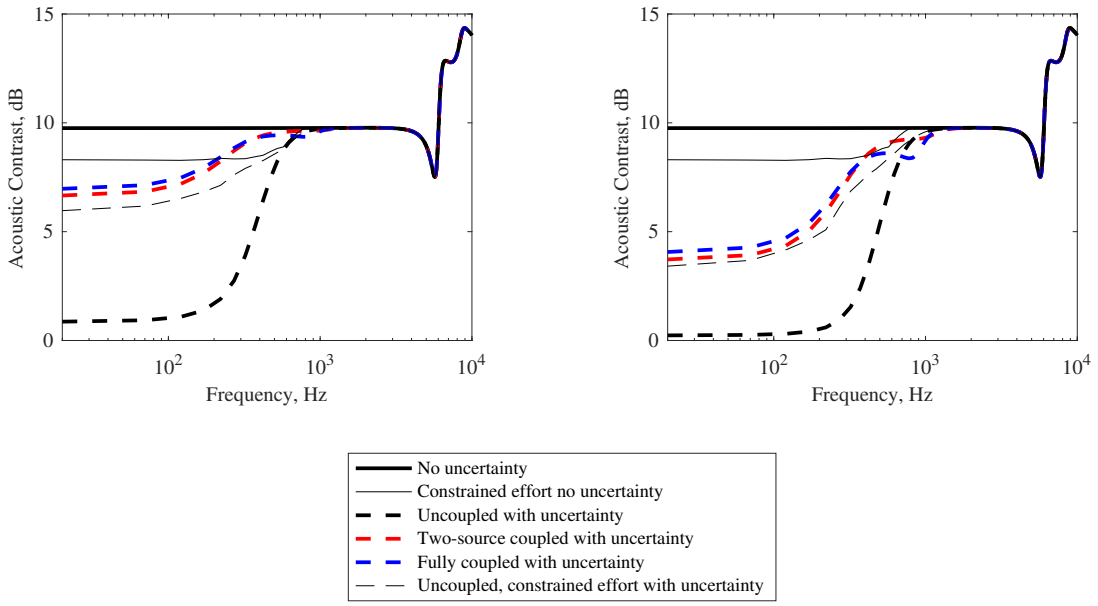

Figure 4: The average acoustic contrast for the dual-layer loudspeaker arrays without uncertainty and no effort constraint (bold solid black line) and with a constraint on the array effort (thin solid black line), and for the uncoupled array (bold dashed black line), two-source coupled array (bold dashed red line), fully coupled array (bold dashed blue line) and uncoupled array with an effort constraint (thin dashed black line) with a normalised rms random variation in the transfer responses of (a) $e = 0.05$ and (b) $e = 0.1$

5. Conclusions

The robustness and efficiency of superdirective arrays used to generate personal sound zones must be considered in practical applications. In general, the robustness and efficiency of such arrays has been controlled through the use of regularisation, however, this results in a reduced acoustic contrast. Previous work has demonstrated that for a two-source endfire array, both the electrical power requirement and robustness to uncertainties can be improved without reducing the acoustic contrast performance by acoustically coupling the two loudspeakers. This paper has described an extension to this work where the effect of acoustic coupling on dual-layer arrays of loudspeakers has been investigated. In this case it is possible to either couple pairs of back-to-back loudspeakers or couple all of the loudspeakers in the array via a single common enclosure. A two-port model of the two coupled arrays and a standard uncoupled array has been presented and using this simulation environment a series of simulation results have been presented. These results have demonstrated that under optimal conditions both coupled arrays achieve the same acoustic contrast as the uncoupled array, but reduce the electrical power required at low frequencies by a factor of 40. It has also be shown that in the presence of response uncertainties, the acoustically coupled arrays are more robust than the uncoupled configuration. These results suggest that the coupled array configurations could provide practical benefits, however, it is also worth highlighting that the additional resonances in these systems may also lead to enclosure resonances that cannot be damped in the usual manner and may, therefore, reduce the audio quality.

REFERENCES

1. Elliott, S. J., Cheer, J., Murfet, H. and Holland, K. R. Minimally radiating sources for personal audio, *The Journal of the Acoustical Society of America*, **128** (4), 1721–1728, (2010).
2. Cheer, J., Elliott, S. J., Kim, Y. and Choi, J.-W. Practical implementation of personal audio in a mobile device, *Journal of the Audio Engineering Society*, **61** (5), 290–300, (2013).
3. Chang, J.-H., Lee, C.-H., Park, J.-Y. and Kim, Y.-H. A realization of sound focused personal audio system using acoustic contrast control, *The Journal of the Acoustical Society of America*, **125** (4), 2091–2097, (2009).
4. Cheer, J., Elliott, S. J. and Gálvez, M. F. S. Design and implementation of a car cabin personal audio system, *Journal of the Audio Engineering Society*, **61** (6), 412–424, (2013).
5. Liao, X., Cheer, J., Elliott, S. and Zheng, S. Design of a loudspeaker array for personal audio in a car cabin, *Journal of the Audio Engineering Society*, pp. 1–12, (2016).
6. Simón Gálvez, M. F., Elliott, S. J. and Cheer, J. A superdirective array of phase shift sources, *The Journal of the Acoustical Society of America*, **132** (2), 746–756, (2012).
7. Elliott, S. J. and Jones, M. An active headrest for personal audio, *The Journal of the Acoustical Society of America*, **119** (5), 2702–2709, (2006).
8. Choi, J.-W. and Kim, Y.-H. Generation of an acoustically bright zone with an illuminated region using multiple sources, *The Journal of the Acoustical Society of America*, **111** (4), 1695–1700, (2002).
9. Poletti, M. An investigation of 2-d multizone surround sound systems, *Audio Engineering Society Convention 125*, Audio Engineering Society, (2008).
10. Chang, J.-H. and Jacobsen, F. Sound field control with a circular double-layer array of loudspeakers, *The Journal of the Acoustical Society of America*, **131** (6), 4518–4525, (2012).
11. Simón Gálvez, M. F., Elliott, S. J. and Cheer, J. Time domain optimization of filters used in a loudspeaker array for personal audio, *IEEE/ACM Transactions on Audio, Speech and Language Processing (TASLP)*, **23** (11), 1869–1878, (2015).
12. Coleman, P., Jackson, P. J., Olik, M. and Abildgaard Pedersen, J. Personal audio with a planar bright zone, *The Journal of the Acoustical Society of America*, **136** (4), 1725–1735, (2014).
13. Elliott, S. J., Cheer, J., Choi, J.-W. and Kim, Y. Robustness and regularization of personal audio systems, *IEEE Transactions on Audio, Speech, and Language Processing*, **20** (7), 2123–2133, (2012).
14. Coleman, P., Jackson, P. J., Olik, M., Møller, M., Olsen, M. and Abildgaard Pedersen, J. Acoustic contrast, planarity and robustness of sound zone methods using a circular loudspeaker array, *The Journal of the Acoustical Society of America*, **135** (4), 1929–1940, (2014).
15. Park, J.-Y., Choi, J.-W. and Kim, Y.-H. Acoustic contrast sensitivity to transfer function errors in the design of a personal audio system, *The Journal of the Acoustical Society of America*, **134** (1), EL112–EL118, (2013).
16. Baykaner, K., Coleman, P., Mason, R., Jackson, P. J., Francombe, J., Olik, M. and Bech, S. The relationship between target quality and interference in sound zone, *Journal of the Audio Engineering Society*, **63** (1/2), 78–89, (2015).
17. Ma, X., Hegarty, P. J., Pedersen, J. A., Johansen, L. G. and Larsen, J. J. Personal sound zones: The significance of loudspeaker driver nonlinear distortion, *Audio Engineering Society Conference: 2016 AES International Conference on Sound Field Control*, Audio Engineering Society, (2016).
18. Zhu, Q., Coleman, P., Wu, M. and Yang, J. Robust personal audio reproduction based on acoustic transfer function modelling, *Audio Engineering Society Conference: 2016 AES International Conference on Sound Field Control*, Audio Engineering Society, (2016).
19. Cheer, J. Robustness and efficiency of an acoustically coupled two-source superdirective array, *22nd International Congress on Sound and Vibration*, (2015).
20. Shin, M., Fazi, F. M., Nelson, P. A. and Hirono, F. C. Controlled sound field with a dual layer loudspeaker array, *Journal of Sound and Vibration*, **333** (16), 3794–3817, (2014).